J|A|C|S
COMMUNICATIONS

Published on Web 04/24/2007

Nanoscale Tunable Proton/Hydrogen Sensing: Evidence for Surface-Adsorbed Hydrogen Atom on Architectured Palladium Nanoparticles

Han-Pu Liang,[†] Nathan S. Lawrence,*[,†] Timothy G. J. Jones,[†] Craig E. Banks,[†] and Caterina Ducati[‡]

Schlumberger Cambridge Research, High Cross, Madingley Road, Cambridge CB3 0EL, U.K., and Department of Materials Science and Metallurgy, University of Cambridge, Pembroke Street, Cambridge CB2 3QZ, U.K.

Received February 2, 2007; E-mail: nlawrenc@cambridge.oilfield.slb.com

Studies on the interaction between metals and hydrogen have attracted increasing attention as driven by the need to use hydrogen as an alternative energy source to relieve greenhouse gas emissions and the energy crisis.[1] Palladium is one of the most attractive metals utilized in the detection of hydrogen gas due to its highly specific interaction with hydrogen and deuterium.[2] However, although highly selective, this important interaction has proven to be complex to understand and, therefore, limits its use in several applications.

The electrochemical response of hydrogen has been studied extensively on palladium macroelectrodes.[3,4] In this case, the hydrogen atoms are essentially absorbed into the Pd lattice. This is a so-called "dissolution adsorption mechanism" in which H^+ ions first adsorb onto the Pd surface and are subsequently reduced to give adsorbed hydrogen (H_{ad}). The adsorbed hydrogen atoms finally diffuse into the bulk Pd such that they lie underneath the first few atomic layers of Pd atoms forming absorbed hydrogen (H_{ab}).[3] Only a single oxidative redox wave is observed encompassing the oxidation of both H_{ab} and H_{ad} to H^+.

Recently, it has been shown that the use of electrodeposited Pd nanoparticles allows the oxidation of both the H_{ad} and H_{ab} to be deconvoluted[5] such that two oxidative waves are observed. This behavior was attributed to the larger ratio of surface to bulk sites at these nanoparticles compared to the Pd macroelectrode. However, in these studies, the size of the nanoparticles was difficult to control, and they were typically around 100 nm or larger. This caused a mixed analytical response to be observed, making sensing problematic.

In the following, we demonstrate the first direct experimental verification that the electrochemical response of the Pd hydrogen system can be controlled. Particularly, the analytical response can be easily tailored in favor of either H_{ad} oxidation or H_{ab} oxidation by nanoscale tuning the coverage of Pd on Au nanoparticles.

The Au/Pd nanostructure is one of the most popular core−shell examples,[6] as the respective lattices of Au and Pd are reasonably similar and, as such, the interfacial energy between them is kept low. This means that, when the Pd nanoparticles form in solution, they are prone to deposit on the Au lattice rather than self-nucleate in solution. In the present study, Au/Pd core−shell nanoparticles are achieved by homogeneously depositing Pd nanoparticles onto Au nanoparticles. This is known as the seeded growth method. The detailed experimental procedure for samples 1−7 can be found in the Supporting Information (Table S1).

Figure 1a shows a scheme detailing the fabrication process of Au/Pd core−shell nanoparticles. Herein, the added Au nanoparticles actually serve as nucleation centers to allow the subsequent deposition process of Pd to take place predominantly at the surface of Au nanoparticles. By delicately decreasing the concentration of H_2PdCl_4 in the reaction mixture, the surface coverage of Pd upon the Au can be effortlessly controlled. Figure 1b gives the X-ray diffraction (XRD) patterns of samples 1, 2, and 4−7, which obviously indicate that the peaks of Pd decrease, while those of Au increase as the H_2PdCl_4 concentration is lowered. This is due to the decreased coverage of Pd on the Au nanoparticles as the amount of Au nanoparticles is kept constant. Typical TEM images (Figure S2) clearly demonstrate that the thickness of Pd shell, that is, Pd coverage or surface roughness, gradually declines with decaying H_2PdCl_4 concentration. Further evidence of the decline of Pd coverage was obtained from UV−vis absorption spectra (Figure S3) and energy dispersive X-ray (EDX) analysis (Figure S4).

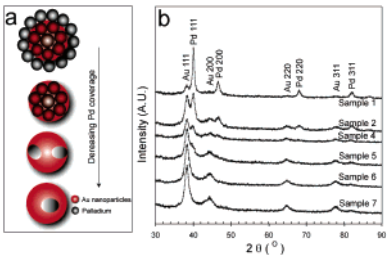

Figure 1. (a) Scheme illustrating the fabrication process of Au/Pd core−shell nanoparticles at different stages by deliberately decreasing the volume of H_2PdCl_4; (b) the X-ray diffraction (XRD) patterns of samples 1, 2, and 4−7.

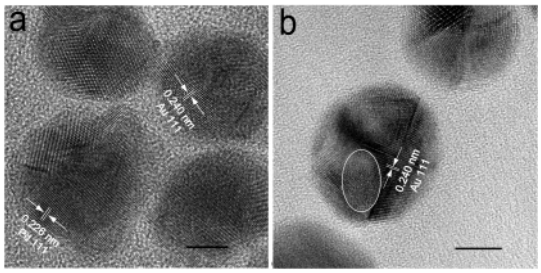

Figure 2. High-resolution transmission electron microscope (HRTEM) image of (a) sample 5 and (b) sample 6. The scale bar in both images is 5 nm.

It is interesting to note that weak Pd shoulder peaks are observed in the XRD patterns of samples 4 and 5, whereas only distinctive Au peaks are observed in samples 6 and 7. This is the key strategy of our experimental design as it is envisaged that by decreasing the volume of H_2PdCl_4 smaller Pd nanoparticles will deposit on the surface of Au nanoparticles. However, this makes identification of the Pd deposit on the Au nanoparticles problematic when using the TEM images of samples 6 and 7 (Figure S2d and e) because the black spots on the spherical Au nanoparticles can be identified as either Pd nanoparticles or as a different crystal plane of Au.

From the HRTEM image of sample 5 in Figure 2a, it is evident that the nanoparticles with an irregular surface are the Au/Pd core−shell nanoparticles whereas the nanoparticles with smooth regular surfaces are Au. Figure 2b shows the HRTEM image of sample 6

[†] Schlumberger Cambridge Research.
[‡] University of Cambridge.

10.1021/ja070760a CCC: $37.00

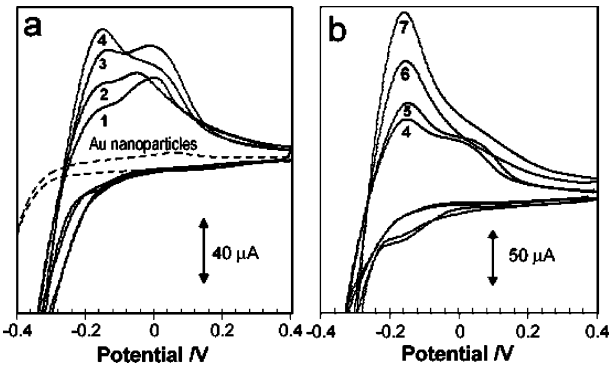

Figure 3. Cyclic voltammetric response (scan rate = 0.1 V·s^{-1}) of (a) the bare Au nanoparticles and samples 1−4 and (b) samples 4−7 of the Au/Pd particles when dispersed on a boron-doped diamond (BDD) electrode and placed in 1 M H_2SO_4. Pd loading for each sample was 0.28 μg.

and illustrates that the free assembly part indicated by the white ellipse can be identified as Pd because it stands on a uniform Au lattice. Consequently, smaller Pd nanoparticles deposited on Au are "flat" rather than spherical. This can be tentatively attributed to the fact that such structures tend to reduce the free energy of the system and, thus, stabilize the newly synthesized bimetallic structure.[6a] The white ellipses shown in the HRTEM image of sample 7 (Figure S5) indicate the places where Pd has possibly deposited onto the Au nanoparticles with no free Pd nanoparticles observed. These results thus show that, by lowering the concentration of H_2PdCl_4 in the reaction mixture, the architecture of the Pd coverage can be manipulated from a complete shell formation (samples 1−5) to an incomplete shell formation with smaller, well-dispersed flat Pd nanostructures (samples 6 and 7) upon the Au nanoparticles.

The interaction of protons with Pd is of significant interest to electrochemists for both the analytical detection of hydrogen and its role in hydrogen storage devices. The ability to chemically manipulate the Pd surface coverage on the Au nanoparticles had a profound effect on the particles' electrochemical response to proton concentration. Figures 3a and b detail the cyclic voltammetric responses (scan rate = 0.1 V·s^{-1}) of both the bare Au nanoparticles and the Au/Pd particles when dispersed on a boron-doped diamond (BDD) electrode and placed in 1 M H_2SO_4. Analysis of Figure 3a reveals that the Au nanoparticles alone show a voltammetric signal with no appreciable oxidative and reductive redox waves; hence, any voltammetric response ascribed below can be solely attributed to the presence of Pd upon the Au. It should be noted that the Pd loading of all samples on the BDD was kept constant for all of the experiments, and therefore, any variation in voltammetric behavior is solely due to the size and surface coverage of Pd on the Au nanoparticles. In all cases, including sample 7, the response of the Au/Pd nanoparticles produced well-defined oxidative signals, thus indicating the presence of Pd in all of the samples.

The response of sample 1 reveals a large increase in the reduction current as the potential is swept negative in contrast to the bare Au nanoparticles. This is consistent with reduction of protons on the Pd layer. Upon reversal of the scan direction, two oxidation waves are observed, the first as a shoulder at −0.15 V and the second main peak at +0.05 V. This is analogous to the response obtained at nanoscale Pd layers[5] in which the wave at +0.05 V is ascribed to the oxidation of H_{ab} and the peak at −0.15 V is oxidation of H_{ad}. Lowering the Pd layer coverage on the Au nanoparticles (samples 2−4, Figure 3a) produces a decrease in the current response at +0.05 V with a concomitant increase at −0.15 V. This trend is further demonstrated by the electrochemical response of samples 4−7 (Figure 3b). As the Pd coverage is lowered, samples 4−7, the H_{ab} peak at +0.05 V decays further while the H_{ad} peak at −0.15 V becomes predominant. Furthermore, in the control experiments, bubbling of N_2 across the electrode surface during the voltammetric cycle gave no variation in the signal. This can be rationalized as follows: lowering of the H_2PdCl_4 concentration in the starting solution produces well-dispersed, flat Pd nanoparticles on the Au (see above). These flat Pd nanoparticles have a large surface area on which the hydrogen atom can adsorb. As the surface coverage decreases, the absorption sites are greatly decreased, allowing the H_{ad} oxidation peak to dominate the cyclic voltammetric response. This is verified by analyzing the charge ratio associated with oxidation of adsorbed ($Q(H_{ad})$) and absorbed hydrogen ($Q(H_{ab})$) with Pd coverage (Figure S6). As the coverage decreases the charge ratio ($Q(H_{ad})/Q(H_{ab})$) is enhanced.

In summary, we have demonstrated that the electrochemical response of hydrogen at Pd is critically dependent on the size and structure of the Pd surface. Evidence has been produced showing that, by manipulating the Pd particle structure to the nanoscale, an electrochemical signal attributed purely to oxidation of adsorbed hydrogen atoms can be achieved due to the large ratio of hydrogen atom adsorption sites compared to the absorption sites. Conversely, the formation of a Pd shell upon a Au nanoparticle allows the response to be dominated by absorbed hydrogen atoms due to the rapid decrease in adsorption to absorption sites. This nanoscale tuning will have significant implications for both hydrogen sensing and hydrogen storage applications.

Acknowledgment. The authors thank Graeme Langlands for conducting the XRD experiments. C.D. wishes to thank the Royal Society for funding.

Supporting Information Available: Detailed experimental procedure, UV/VIS, SEM, TEM, EDX, and HRTEM. This material is available free of charge via the Internet at http://pubs.acs.org.

References

(1) (a) Dresselhaus, M. S.; Thomas, I. L. *Nature* **2001**, *414*, 332−337. (b) Ward, M. D. *Science* **2003**, *300*, 1104−1105. (c) Schlapbach, L.; Züttel, A. *Nature* **2001**, *414*, 353−358. (d) Special section on Toward A Hydrogen Economy *Science* **2004**, *305*, 957−974. (e) Fernandez, J. L.; Raghuveer, V.; Manthiram, A.; Bard, A. J. *J. Am. Chem. Soc.* **2005**, *127*, 13100−13101.

(2) (a) Lewis, F. A. *The Palladium-Hydrogen System*; Academic Press: London, 1967. (b) Favier, F.; Walter, E. C.; Zach, M. P.; Benter, T.; Penner, R. M. *Science* **2001**, *293*, 2227−2231. (c) Walter, E. C.; Favier, F.; Penner, R. M. *Anal. Chem.* **2002**, *74*, 1546−1553.

(3) (a) Breiter, M. W. *J. Electroanal. Chem.* **1980**, *109*, 253−260. (b) Breiter, M. W. *J. Electroanal. Chem.* **1977**, *81*, 275−284. (c) Mengoli, G.; Fabrizio, M.; Manduchi, C.; Zannoni, G. *J. Electroanal. Chem.* **1993**, *350*, 57−72.

(4) (a) Horkans, J. *J. Electroanal. Chem.* **1980**, *106*, 245−249. (b) McBreen, J. *J. Electroanal. Chem.* **1990**, *287*, 279−291. (c) Andreasen, G.; Visintin, A.; Salvarezza, R. C.; Triaca, W. E.; Arvia, A. J. *Langmuir* **1999**, *15*, 1−5. (d) Enyo, M. *J. Electroanal. Chem.* **1982**, *134*, 75−86. (e) Paillier, J.; Roue, L. *J. Electrochem. Soc.* **2005**, *152*, E1−E8. (f) Lukaszewski, M.; Kusmierczyk, K.; Kotowski, J.; Siwek, H.; Czerwinski, A. *J. Solid State Electrochem.* **2003**, *7*, 69−76. (g) Gabrielli, C.; Grand, P. P.; Lasia, A.; Perrot, H. *J. Electrochem. Soc.* **2004**, *151*, A1937−A1942. (h) Baldauf, M.; Kolb, D. M. *Electrochim. Acta* **1993**, *38*, 2145−2153.

(5) (a) Gimeno, Y.; Hernandez Creus, A.; Gonzalas, S.; Salvarezza, R. C.; Arvia, A. J. *Chem. Mater.* **2001**, *13*, 1857−1864. (b) Batchelor-McAuley, C.; Banks, C. E.; Simm, A. O.; Jones, T. G. J.; Compton, R. G. *ChemPhysChem* **2006**, *7*, 1081−1085.

(6) (a) Rodríguez-López, J. L.; Montejano-Carrizales, J. M.; Pal, U.; Sánchez-Ramírez, J. F.; Troiani, H. E.; García, D.; Miki-Yoshida, M.; José-Yacamán, M. *Phys. Rev. Lett.* **2004**, *92*, Art. No. 196102. (b) Xiang, Y. J.; Wu, X. C.; Liu, D. F.; Jiang, X. Y.; Chu, W. G.; Li, Z. Y.; Ma, Y.; Zhou, W. Y.; Xie, S. S. *Nano Lett.* **2006**, *6*, 2290−2294. (c) Lu, L. H.; Wang, H. S.; Xi, S. Q.; Zhang, H. J. *J. Mater. Chem.* **2002**, *12*, 156−158. (d) Ge, Z.; Cahill, D. G.; Braun, P. V. *J. Phys. Chem. B* **2004**, *108*, 18870−18875. (e) Kim, J.-H.; Chung, H.-W.; Lee, T. R. *Chem. Mater.* **2006**, *18*, 4115−4120. (f) Fujimoto, T.; Nagata, Y.; Oshima, R.; Maeda, Y. *J. Phys. Chem. B* **2000**, *104*, 6028−6032.

JA070760A